

# Polarization and strain response in $\text{Bi}_{0.5}\text{K}_{0.5}\text{TiO}_3$ - $\text{BiFeO}_3$ ceramics

Maxim. I. Morozov, Mari-Ann Einarsrud, and Tor Grande

*Department of Materials Science and Engineering, Norwegian University of Science and Technology, NO-7491 Trondheim,*

Highly dense and phase-pure ferroelectric ceramics in the  $(1-x)\text{Bi}_{0.5}\text{K}_{0.5}\text{TiO}_3 - x\text{BiFeO}_3$  system have been prepared and examined in a wide range of composition ( $0.1 \leq x \leq 0.9$ ). The dielectric and electromechanical properties have been shown to reach a maximum value at  $x \approx 0.25$  demonstrating a high strain performance (250 – 370 pm/V in the temperature range 25 – 175 °C). Stability of the strain response with respect to temperature, as well as frequency and amplitude of the driving electric field is reported and discussed.

Perovskite ceramics based on mixed bismuth and alkali A-cations form a group of prominent lead-free piezoelectric alternatives whose potential is not fully explored yet.<sup>1,2</sup> Bismuth potassium titanate,  $\text{Bi}_{0.5}\text{K}_{0.5}\text{TiO}_3$  (BKT), and bismuth ferrite,  $\text{BiFeO}_3$  (BFO), are ferroelectrics with relatively high Curie temperatures ( $T_C$ ): above 370 °C,<sup>3-5</sup> and above 820 °C,<sup>6,7</sup> respectively. Both materials have been reported to be challenging to prepare by the conventional ceramic processing. Fabrication of BKT typically meets problems with densification<sup>8</sup> and phase purity,<sup>5,8-11</sup> which are suggested to originate from high volatility of potassium and bismuth at the sintering temperatures, although fabrication of phase pure BKT ceramics by the traditional solid-state reaction method has recently been reported.<sup>12</sup> BFO is a metastable compound with respect to

the parasitic neighbor phases at the intermediate temperature range,<sup>13</sup> and thus known as a challenging material to fabricate in single phase state.

Dielectric and piezoelectric properties of BKT have been intensively studied<sup>3,5,8-12</sup> and known to be moderate ( $\epsilon_r \approx 770$ ,  $d_{33} \approx 80 - 100$  pC/N,  $S_{\max}/E_{\max} \approx 130$  pm/V),<sup>1</sup> though texturing<sup>14</sup> or various modifiers<sup>1</sup> may serve for improvement.

For a long time BFO has been known as a ferroelectric with relatively low dielectric and piezoelectric properties ( $\epsilon_r \approx 30$ ,<sup>15</sup>  $d_{33} \approx 50 - 70$  pm/V,<sup>16</sup>  $S_{\max}/E_{\max} \approx 117$  pm/V<sup>17</sup>). Lately, the material has been intensively studied as the only known compound exhibiting multiferroism at room temperature.<sup>18</sup> Recently, a very high strain response has been observed in BFO under extra-high electric field (E-field) amplitudes (peak-to-peak strain of 0.36 % at 140 kV/cm in bulk ceramics<sup>19</sup> and above 5 % at 1.5 MV/cm in thin films<sup>20</sup>), which gave rise to consideration of BFO's piezoelectric potential in future lead-free applications.

The dielectric and piezoelectric properties of ceramics in some limited ranges of BKT-BFO solid solutions have recently appeared in sole publications.<sup>21,22</sup> Matsuo et al.<sup>21</sup> reported the properties of  $(1-x)\text{BKT} - x\text{BFO}$  ceramics in the range  $0.4 \leq x \leq 0.8$ , while the range  $0 \leq x \leq 0.4$  was investigated by Kim et al.<sup>22</sup> Attempts to prepare BKT-BFO ceramics by the solid-state reaction method met the same difficulties as mentioned above for pure BKT and BFO. Ceramics prepared by the conventional sintering method did not exceed 90% of theoretical density<sup>21</sup> and formation of secondary phases was reported for  $x \geq 0.1$ .<sup>22</sup>

A complementary analysis of the crystal and domain structures in these ceramics showed the presence of a morphotropic phase boundary (MPB) at  $x \approx 0.6$  between the polar rhombohedral phase R3c and a pseudocubic phase consisting of locally disordered lattice with non-polar cubic and polar rhombohedral nanodomain structure.<sup>23</sup> However, the dielectric and piezoelectric properties characterized as a function of composition showed rather ambiguous

behavior with respect to the MPB. Some features of the P-E loops such as coercive field  $E_C$  and remanent polarization  $P_r$ , as well as the effective piezoelectric strain coefficient  $d_{33}^*$ , displayed an apparent maximum at MPB, while no marked enhancement was observed for the E-field induced strain  $S_{\max}/E_{\max}$  and the relative dielectric permittivity  $\epsilon_r$ .<sup>21</sup> Let us note that the full opening of hysteresis loops, and hence, their parameters  $E_C$  and  $P_r$  may be strongly influenced by several secondary factors such as unstable long-range polar order in relaxors, different mechanisms of domain wall pinning, leakage current, available range of the driving E-field amplitude, etc. In turn, the measured small signal parameter  $d_{33}^*$  strongly depends on  $P_r$ , i.e. on sufficient poling and ability of the ferroelectrics to keep the remanent polarization after the poling cycle. On the other hand, BKT has tetragonal ( $P4mm$ ) structure<sup>4</sup> and thus, in case of unlimited solubility of BKT and BF, another phase boundary separating the *tetragonal* phase and the reported in Ref.<sup>21,23</sup> *pseudocubic* phase with polar *rhomboidal* nanodomains can be anticipated. A tendency of reducing tetragonal lattice distortion with increasing BFO content was reported in Ref.<sup>22</sup>, where the BKT side of the system was examined.

In this letter we report an attempt to find and investigate the composition exhibiting the highest dielectric and electromechanical properties in the BKT-BFO system. For this purpose phase-pure and dense  $(1-x)\text{BKT} - x\text{BFO}$  ceramics were fabricated and examined within the wide range of compositions  $0.1 \leq x \leq 0.9$ . In contrast to the previous study,<sup>21</sup> we applied low or moderate amplitudes of electric field for characterization of the dielectric and strain response in order to exclude influence of possible domain wall pinning-depinning processes induced by strong E-field amplitude on the measured properties.

The ceramics under study were prepared by the conventional solid state reaction method using high-purity and fine-grade oxide and carbonate precursors. The phase purity and high relative density (97 - 98 %) was achieved by careful adjustment of milling, calcination, and sintering regimes. A more detailed report on preparation and preliminary characterization of the

ceramic displaying the highest electromechanical performance in the BKT-BFO system is reported elsewhere.<sup>24</sup>

The X-Ray diffraction patterns taken from the mechanically grounded and polished surfaces of bulk ceramics are shown in Fig.1. All the patterns can be indexed to a single phase with perovskite type structure. As reported in Refs.<sup>21,23</sup>, a structural phase boundary at  $x \approx 0.6$  takes place in the system. It can be recognized by the vanishing diffraction line  $(113)_{R3c}$  and the splitting of the  $(111)_C$  reflection. On the potassium-rich side, the tetragonal splitting of the  $(100)_C$  and  $(200)_C$  reflections vanishes by approaching  $x \approx 0.25$ , and transforms to a shoulder that remains for compositions with higher BFO content. Taking into account this feature, it is reasonable to anticipate that a *pseudo-cubic* phase with disordered lattice consisting of both *non-polar* and *polar tetragonal* nanodomains may also exist in the system somewhere close to the potassium-rich side of the system. Note, that BKT itself, as relaxor ferroelectric,<sup>5,8</sup> exhibits such boundary at temperature  $T_m \approx 280$  °C, where the *polar tetragonal* structure gradually changes upon heating to the *cubic* state with some *polar tetragonal* areas persisting up to 400 °C.<sup>4,25</sup> Finally, refinement of the patterns using the space groups of the two end members or a *cubic* perovskite was challenging due to peak broadening and strain effects. Further evaluation of the corresponding XRD powder patterns is underway.

Fig. 2 shows the E-field induced strain and polarization hystereses for the  $(1-x)\text{BKT} - x\text{BFO}$  ceramics with  $0.1 \leq x \leq 0.7$ . No loop's opening was observed for  $x \geq 0.7$  under the applied field conditions (amplitude  $E_0 = 50$  kV/cm, 0.25 Hz). A gradual transformation of the loops clearly demonstrates the presence of a maximum at  $x \approx 0.25$  for piezoelectric and ferroelectric performance. Interestingly, the shapes of the P-E hysteresis loops shown in Fig. 2(d) differ from the loops reported by Matsuo *et al.*<sup>21</sup> for the same compositions. This is likely an effect of different E-field amplitudes. In our study, an amplitude of 50 kV/cm was high enough to enable the domain switching processes and provide the strain response in ceramics with  $x \leq 0.6$ , while it

was not sufficient for full opening of the P-E hysteresis loops. An incomplete opening of the hysteresis loops may be due to various domain pinning mechanisms, as in the case of BiFeO<sub>3</sub>.<sup>17</sup> We also examined our ceramics under higher electric fields, up to 100 kV/cm, and the observed P-E loops were in good qualitative and quantitative agreement with the previous work.<sup>21</sup> In particular, the P-E loop for the composition  $x = 70$  opened under  $E_0 \geq 70$  kV/cm. However, this range of the E-field amplitudes may still be insufficient for reliable study of the switching processes in the system, especially on the BFO side. For example, observation of the P-E loops opening in BFO ceramics required application of electric fields as high as 150 kV/cm.<sup>17,20</sup> Thus, no observations of opened P-E loops for the compositions with  $x \geq 0.8$  in Ref.<sup>21</sup>, as well as in the present study, may be explained by the limited range of applied electric field.

To ascertain the existence of a maximum in dielectric response at  $x \approx 0.25$  for the  $(1-x)\text{BKT} - x\text{BFO}$  system, the relative dielectric permittivity ( $\epsilon_r$ ) was measured under commonly used characterization conditions (ac peak voltage 1 V, frequency 100 kHz, room temperature) for all the samples in the composition range studied. The result is shown in Fig. 3, which confirms the existence of a maximum in  $\epsilon_r$  at  $x \approx 0.25$  and shows a clear trend in good agreement with previous reports.<sup>5,17,21</sup>

The presence of a maximum in the dielectric and piezoelectric response at  $x \approx 0.25$  suggests possible existence of a structural phase boundary separating the *pseudocubic* phase with local *polar rhombohedral* nanodomains, on the BFO-side, with a similar *pseudocubic* phase with *polar tetragonal* nanodomains or with *tetragonal* phase  $P4mm$ , on the BKT-side of the BKT-BFO system. The presence of *polar tetragonal* nanodomains in this system would require a special structural analysis which has not been addressed yet.

Enhancement of the dielectric and strain response at a boundary between the *tetragonal* and *pseudocubic* phases is quite common in lead-free systems,<sup>2,26-28</sup> though not always the case.<sup>12</sup>

Since the high E-field induced strain makes these lead-free ceramics prospective for actuator application, we consider next the stability of the functional response with respect to temperature, frequency, and amplitude of the driving electric field. The unipolar strain response in three samples of 0.75BKT-0.25BFO (BKTF-25) ceramics was measured under two different polarities as a function of three independent measurement variables (temperature, frequency, and E-field amplitude). The results are shown in Fig. 4. The strain response measured at a fixed E-field amplitude (50 kV/cm) and frequency ( $\sim 0.5$  Hz) increases with increasing temperature from  $\sim 250$  pm/V up to  $\sim 370$  pm/V at  $100^\circ\text{C}$  and stabilizes at higher temperatures (Fig. 4(a)). This is in qualitative agreement with our preliminary characterization, though the averaged strain derived in this work is slightly higher than in our previous report.<sup>24</sup> The frequency dispersion of the strain also shows a stable response above  $100^\circ\text{C}$ , while logarithmic frequency dependence takes place at room temperature (Fig. 4(b)). Finally, the optimal range of the driving E-field amplitudes is found to be above 50 kV/cm at ambient and slightly decreasing with increasing temperature (Fig. 4(c)).

The origin of the observed dispersion in the strain response can be rationalized considering two possible contributions. The first contribution is related to a possible presence of ferroelastic domains, whose frequency dependent contribution seemingly vanishes above  $100^\circ\text{C}$ . The frequency dependent manifestation of domain wall dynamics<sup>29</sup> is well-known for lead-based ferroelectric ceramics.<sup>30-32</sup>

However, the frequency dispersion of strain observed in the BKTF-25 ceramics at room temperature (Fig. 4(a)) is much stronger than in the abovementioned lead-based ferroelectrics and rather comparable with that observed in lead-based<sup>33</sup> and lead-free<sup>34</sup> relaxors. The temperature-dependent dielectric dispersion in the BKT-BFO system is relaxor-like,<sup>21,22</sup> including the case of BKTF-25.<sup>24</sup> Thus, the second possible contribution may be related to some extent of ergodicity, when the field-induced long-range polar order in relaxor is partially unstable.<sup>34</sup> Such assumption

is consistent with low piezoelectric coefficients  $d_{33} < 50$  pC/N reported for  $(1-x)\text{BKT} - x\text{BFO}$  compositions with  $0.1 < x < 0.5$ .<sup>21,22</sup> Formation of the long-range polar order and its ferroelectric and piezoelectric manifestations in relaxor ferroelectrics can be, at least in part, induced by an applied electric field during the measurement cycle. This process, in general, contributes as an additional delay in the strain response. Indeed, the unipolar strains at room temperature show frequency dependent amplitudes and hysteretic shapes (Fig. 5(a)). At higher temperature, essentially above 100 °C, this effect almost disappears (Fig. 5 (b)), thus suggesting that the E-field induced ferroelectric order forms faster or does not form at all.

In order to elucidate the mechanisms contributing to the electromechanical response at ambient and with increasing temperature, the hysteretic responses in the BKTF-25 ceramics are compared in Fig. 6 for the two contrasting cases: (1) low frequency and low temperature and (2) high frequency (mainly to avoid *dc*-leakage) and high temperature. The presence of both the polarization reversal and the negative strain in the first case indicates existence of a long-range ferroelectric order and its piezoelectric contribution to the total strain. In the second case, the observed polarization hysteresis indicates that a long-range ferroelectric order with the polarization reversal still retains at 200 °C, while its ferroelastic manifestation is minor, as only positive strain was induced by bipolar E-field cycle. Thus, the higher the temperature is, the more electrostrictive in nature is the strain response of the BKTF-25 ceramics.

In summary, phase pure and dense  $(1-x)\text{BKT} - x\text{BFO}$  ceramics were prepared and examined in a wide range of composition  $0.1 \leq x \leq 0.9$ . The dielectric and electromechanical properties in this system display a pronounced maximum at  $x \approx 0.25$ . Thus a structural phase boundary may be anticipated at this composition. The ceramics with  $x \approx 0.25$  demonstrated a high magnitude of the E-field induced strain with appreciable frequency and temperature stability above 100 °C, where the strain response is mainly electrostrictive. This material is therefore a promising lead-free alternative for actuator applications

## References

- <sup>1</sup>J. Rödel, W. Jo, K. T. P. Seifert, E.-M. Anton, T. Granzow, and D. Damjanovic, *J. Am. Ceram. Soc.*, **92**, 1153 (2009).
- <sup>2</sup>S. Leontsev and R. E. Eitel, *Sci. Technol. Adv. Mater.*, **11**, 044302 (2010).
- <sup>3</sup>C. F. Buhrer, *J. Chem. Phys.*, **36**, 798 (1962).
- <sup>4</sup>V. V. Ivanova, A. G. Kapyshev, Y. N. Venevtsev, and G. S. Zhdanov, *Izv. Akad. Nauk SSSR* **26**, 354 (1962).
- <sup>5</sup>Y. Hiruma, R. Aoyagi, H. Nagata, and T. Takenaka, *Jap. J. Appl. Phys.* **44**, 5040 (2005)
- <sup>6</sup>S. A. Fedulov, *Doklady Akademii Nauk Sssr*, **139**, 1345(1961).
- <sup>7</sup>M. M. Kumar, V. R. Palkar, K. Srinivas, and S. V. Suryanarayana, *Appl. Phys. Lett.* **76**, 2764 (2000).
- <sup>8</sup>T. Wada, A. Fukui, and Y. Matsuo, *Jpn. J. Appl. Phys.* **41**, 7025 (2002).
- <sup>9</sup>Z. F. Li, C. L. Wang, W. L. Zhong, J. C. Li, and M. L. Zhao, *J. Appl. Phys.* **94**, 2548 (2003).
- <sup>10</sup>S. C. Zhao, G. R. Li, A. L. Ding, T. B. Wang, and Q. R. Yin, *J. Phys. D* **39**, 2277 (2006).
- <sup>11</sup>Y. D. Hou, L. Hou, S. Y. Huang, M.K. Zhu, H. Wang, and H. Yan, *Solid State Commun.* **137**, 658 (2006).
- <sup>12</sup>L. Martín-Arias, A. Castro, and M. Algueró, *J. Mater. Sci.* **47**, 2729 (2012).
- <sup>13</sup>S. M. Selbach, M.-A. Einarsrud, and T. Grande, *Chem. Mater.* **21**, 169(2009).
- <sup>14</sup>H. Nagata, M. Saitoh, Y. Hiruma, and T. Takenaka, *Jap. J. Appl. Phys.* **49**, 09MD08 (2010).
- <sup>15</sup>S. Kamba, D. Nuzhnyy, M. Savinov, J. Šebek, J. Petzelt, J. Prokleška, R. Haumont, and J. Kreisel, *Phys. Rev. B* **75**, 024403 (2007).
- <sup>16</sup>V. V. Shvartsman, W. Kleemann, R. Haumont, and J. Kreisel, *Appl. Phys. Lett.* **90**, 172115 (2007)



- <sup>17</sup>T. Rojac, M. Kosec, B. Budic, N. Setter, and D. Damjanovic, *J. Appl. Phys.*, **108**, 074107 (2010).
- <sup>18</sup>G. Catalan and J. F. Scott, **21**, 1 (2009).
- <sup>19</sup>J. X. Zhang, B. Xiang, Q. He, J. Seidel, R. J. Zeches, P. Yu, S. Y. Yang, C. H. Wang, Y.-H. Chu, L. W. Martin, A. M. Minor, and R. Ramesh, *Nat. Nanotech.* **6**, 98 (2011)
- <sup>20</sup>T. Rojac, M. Kosec, and D. Damjanovic, *J. Am. Ceram. Soc.* **94**, 4108 (2011).
- <sup>21</sup>H. Matsuo, Y. Noguchi, M. Miyayama, M. Suzuki, A. Watanabe, S. Sasabe, T. Ozaki, S. Mori, S. Torii, and T. Kamiyama, *J. Appl. Phys.* **108**, 104103 (2010).
- <sup>22</sup>J. M. Kim, Y. S. Sung, J.H. Cho, T. K. Song, M. H. Kim, H.H. Chong, T. G. Park, D. Do, and S. S. Kim, *Ferroelectrics* **404**, 88 (2010).
- <sup>23</sup>T. Ozaki, H. Matsuo, Y. Noguchi, M. Miyayama, and S. Mori, *Jap. J. Appl. Phys.* **49**, 09MCO5 (2010).
- <sup>24</sup>M. Morozov, M.-A. Einarsrud, T. Grande, and D. Damjanovic, *Ferroelectrics*, *in print* (2012)
- <sup>25</sup>M. Otonicar, S. D. Skapin, B. Jancar, R. Uvic, and D. Suvorov, *J. Am. Ceram. Soc.* **93**, 4168 (2010).
- <sup>26</sup>S. Leontsev and R. E. Eitel, *J. Am. Ceram. Soc.* **92**, 2957 (2009).
- <sup>27</sup>I. Fujii, R. Mitsui, K. Nakashima, N. Kumada, M. Shimada, T. Watanabe, J. Hayashi, H. Yabuta, M. Kubota, T. Fukui, and S. Wada, *Jap. J. Appl. Phys.* **50**, 09ND07 (2011).
- <sup>28</sup>I. Fujii, K. Nakashima, N. Kumada, and S. Wada, *J. Ceram. Soc. Jap.* **120**, 30 (2012).
- <sup>29</sup>W. Kleemann, *Annu. Rev. Mater. Res.* **37**, 415 (2007)
- <sup>30</sup>Y. H. Chen and D. Viehland, *Appl. Phys. Lett.* **77**, 133 (2000).
- <sup>31</sup>D. Viehland and Y.H. Chen, *J. Appl. Phys.* **88**, 6696 (2000).
- <sup>32</sup>Y. Gao, K. Uchino, and D. Viehland, *J. Appl. Phys.* **92**, 2094 (2002).
- <sup>33</sup>Q. M. Zhang, S.J. Jang, and L. E. Cross, *J. Appl. Phys.* **65**, 2807 (1989).
- <sup>34</sup>R. Dittmer, W. Jo, E. Aulbach, T. Granzow, and J. Rödel, *J. Appl. Phys.* **112**, 014101 (2012).

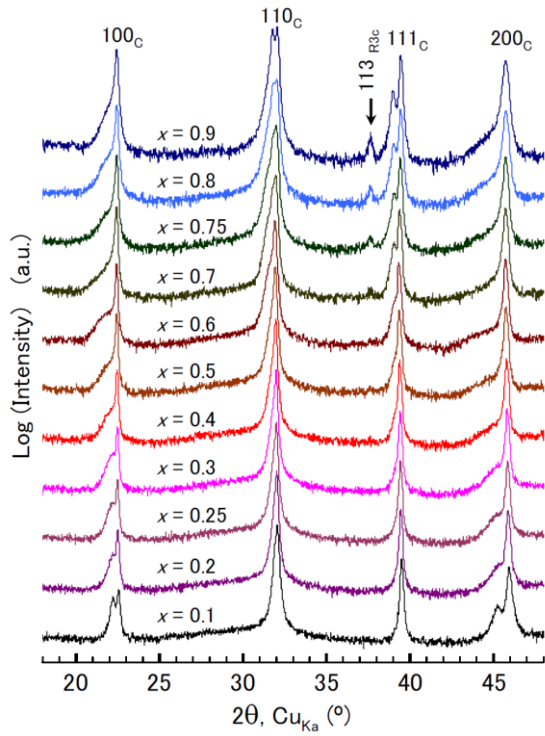


FIG. 1. (Color online) X-Ray diffraction patterns of sintered  $(1-x)\text{BKT} - x\text{BFO}$  ceramics.

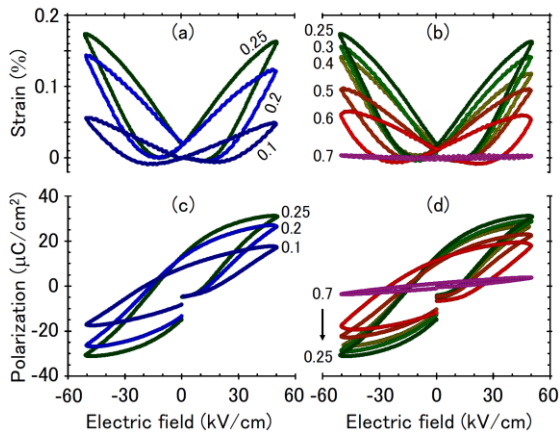


FIG. 2. (Color online) Bipolar strain (a,b) and polarization (c,d) hysteresis loops for various compositions of  $(1-x)\text{BKT} - x\text{BFO}$  ceramics ( $0.1 \leq x \leq 0.7$ ).

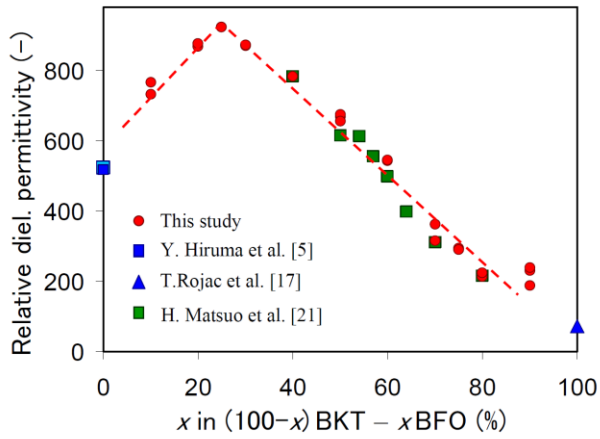


FIG. 3. (Color online) Relative dielectric permittivity as a function of composition in  $(1-x)\text{BKT} - x\text{BFO}$  system. References:  $\text{BKT}^5$ ,  $\text{BFO}^{17}$ ,  $0.4 \leq x \leq 0.8$ .<sup>21</sup>

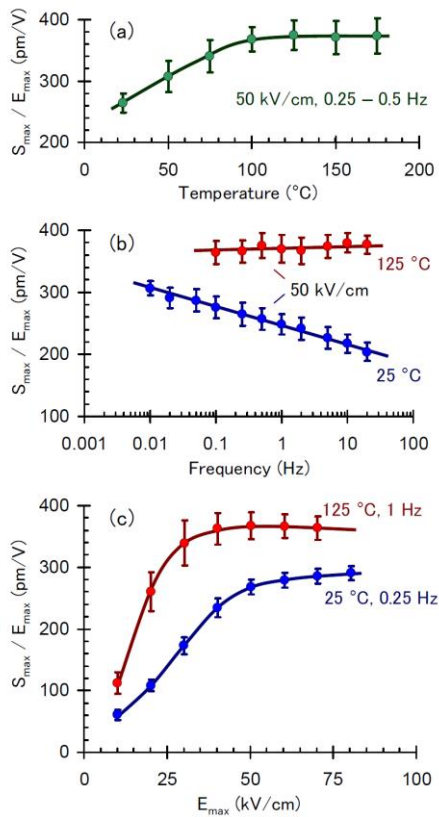


FIG. 4. (Color online) Unipolar electric field-induced strain in BKTF-25 ceramics at various regimes: a) temperature; b) frequency; and c) electric field amplitude dependencies. The data points correspond to the mean values and error bars to one standard deviation.

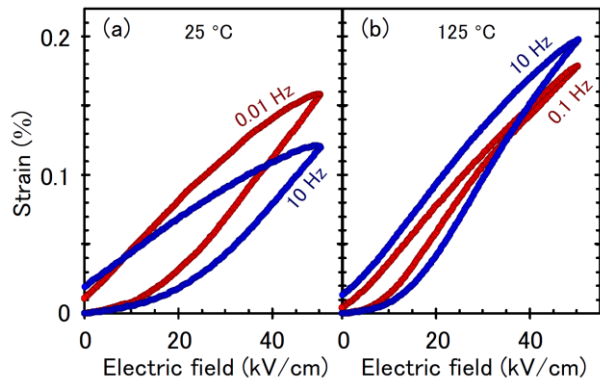


FIG. 5. (Color online) Unipolar electric field-induced strain in BKTF-25 ceramics at different frequency and temperature regimes: a) 25 °C and b) 125 °C

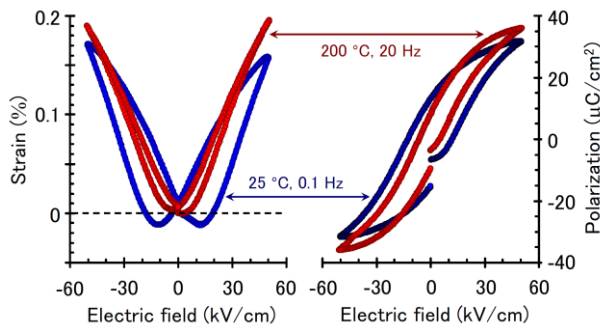


FIG. 6. (Color online) Bipolar electric field-induced strain (left) and polarization (right) response of BKTF-25 ceramics at 25 °C, 0.1 Hz and 200 °C, 20 Hz